

Structural Health Diagnosis and Prognostics Using Fatigue and Crack Growth Monitoring

Daniel Kujawski, Muralidhar K. Ghantasala, Subash Gokanakonda and Shabbir Hussain*

Department of Mechanical and Aeronautical Engineering, Western Michigan University

1903, West Michigan Avenue, Kalamazoo-49008, USA

*TARDEC, 6501 E. 11 Mile Road, Warren, MI 48397-5000

Abstract

Fatigue damage sensing and crack propagation monitoring of any structure is a prerequisite for reliable and effective structural health monitoring. This paper, discusses the role of two different sensors, i.e., crack propagation (CP) and fatigue damage (FD) sensors in structural health monitoring. The CP sensor is capable of detecting crack initiation and subsequent propagation within the structural component that essentially constitutes a diagnostics approach. The FD sensor monitors the actual fatigue damage of the structural component and can be used for both diagnosis and prognosis of the remaining useful life.

The CP sensor bonded to a structure at the critical location monitors the progression of a surface crack breaking through the successive strands, resulting in an increase in total resistance of the FD sensor having alternate slots and strips with different strain magnification factor with respect to the nominal strain at its location. The sensor is designed such that the strips experience the strains which closely resemble the actual strain distribution in the critical area of the component. One of the major advantages of this sensor is that it can be placed at any convenient location, still experiencing the same fatigue damage as a critical location. An interesting aspect of these sensors is that they are easily integrated with wireless networking, facilitating ease of use and real time data acquisition. Both sensors could be applied to various structures from ground civilian and military vehicles to steel bridges. This can predict the remaining useful life of a component or the number of miles (for any automobile) left for the component before it needed replacement.

Report Documentation Page

Form Approved
OMB No. 0704-0188

Public reporting burden for the collection of information is estimated to average 1 hour per response, including the time for reviewing instructions, searching existing data sources, gathering and maintaining the data needed, and completing and reviewing the collection of information. Send comments regarding this burden estimate or any other aspect of this collection of information, including suggestions for reducing this burden, to Washington Headquarters Services, Directorate for Information Operations and Reports, 1215 Jefferson Davis Highway, Suite 1204, Arlington VA 22202-4302. Respondents should be aware that notwithstanding any other provision of law, no person shall be subject to a penalty for failing to comply with a collection of information if it does not display a currently valid OMB control number.

1. REPORT DATE 12 APR 2011	2. REPORT TYPE N/A	3. DATES COVERED -	
4. TITLE AND SUBTITLE Structural Health Diagnosis and Prognostics Using Fatigue and Crack Growth Monitoring		5a. CONTRACT NUMBER	
		5b. GRANT NUMBER	
		5c. PROGRAM ELEMENT NUMBER	
6. AUTHOR(S) Daniel Kujawski; Muralidhar K. Ghantasala; Subash Gokanakonda; Shabbir Hussain		5d. PROJECT NUMBER	
		5e. TASK NUMBER	
		5f. WORK UNIT NUMBER	
7. PERFORMING ORGANIZATION NAME(S) AND ADDRESS(ES) Department of Mechanical and Aeronautical Engineering Western Michigan University 1903 West Michigan Avenue, Kalamazoo, MI 49008, USA US Army RDECOM-TARDEC 6501 E 11 Mile Rd Warren, MI 48397-5000, USA		8. PERFORMING ORGANIZATION REPORT NUMBER 21293RC	
		9. SPONSORING/MONITORING AGENCY NAME(S) AND ADDRESS(ES) US Army RDECOM-TARDEC 6501 E 11 Mile Rd Warren, MI 48397-5000, USA	
10. SPONSOR/MONITOR'S ACRONYM(S) TACOM/TARDEC/RDECOM		11. SPONSOR/MONITOR'S REPORT NUMBER(S) 21293RC	
		12. DISTRIBUTION/AVAILABILITY STATEMENT Approved for public release, distribution unlimited	
13. SUPPLEMENTARY NOTES Presented at SAE 2011 World Congress April 12-14, 2011 Detroit, Michigan, USA, The original document contains color images.			
14. ABSTRACT			
15. SUBJECT TERMS			
16. SECURITY CLASSIFICATION OF:			17. LIMITATION OF ABSTRACT SAR
a. REPORT unclassified	b. ABSTRACT unclassified	c. THIS PAGE unclassified	
18. NUMBER OF PAGES 20			19a. NAME OF RESPONSIBLE PERSON

Introduction

Fatigue has been known to be one of the common causes of failures of multitude of structural components. The fatigue process generally starts with microscopic defects or imperfections in the material of the structure under certain circumstances where they continue to grow and interfuse from macroscopic defects substantially in the form of cracks [1-2]. The growth of thus formed macroscopic defects occurs in the proximity of intense stress concentration zones such as holes, notches etc. [3].

Majority of the structures when subjected to repeated cyclic loadings, experience varying levels of stresses for different number of loading cycles. Thus the fatigue life of a structure depends on its individual stress history. Normally, the S-N approach and certain empirical rules are used to predict the service fatigue life. These empirical rules commonly referred to as cumulative damage rules have also been found inadequate [4]. The cumulative fatigue damage cannot be determined by non-destructive testing or detailed microscopic study of the structure at any given time during the operation of the structure. Further, designing a structure cannot take into account the real service loading, as the actual loading conditions cannot be accurately known *apriori*.

Inspection techniques currently employed involves complex, time-consuming inspection procedures, which can be very labor-intensive and expensive. Parts may have to be disassembled and re-assembled for inspection, which can result in significant equipment downtime. Therefore, there is an urgent need for a faster and more efficient structural health monitoring technique, which at the same time capable of providing a reliable estimate of the remaining fatigue life. This helps in planning or organizing repair / replacement schedule of a given component and thereby minimizing any catastrophic consequences. Hence, a novel fatigue sensor that is useful for structural health monitoring is designed. This paper describes the principle of the dedicated fatigue monitoring sensor along with some preliminary design and simulation results that would show the validity of the concept.

Though few fatigue sensors [7-15] were proposed in the past, each has its own limitations with respect to their operation. Certain kind of crack detection gages have also been developed in the past [17], but they are limited in a way that these crack gages have to be placed at the critical

stress concentration zone on the component where the cracks generate and propagate through such crack gages. These cracks have an array of thin strands and the gage is placed such that the crack generated propagate through the strands and thereby cutting each of the strands successively. Some of the devices are just limited to the measurement of the crack length in the structure, others work in such a way that the fatigue measurement may not be a direct method but it involves a multi-step procedure while some devices give the fatigue life of the structural members through comparing with a series of laboratory experiments.

Hence, a novel fatigue sensor that is useful for structural health monitoring is designed. This paper describes the concept of the dedicated fatigue monitoring sensor along with some preliminary design and simulation results that would show the validity of the working principle of the same. The operation and functionality of the fatigue sensor is discussed in the context of existing crack detection sensors used for structural health diagnosis.

Concept of Fatigue Sensor

The concept of the fatigue sensor is based on the strain life characteristics of the engineering materials. The sensor under consideration consists of alternate slots and strips (ligaments) having different strain magnification factors with respect to the nominal or reference strain. The sensor is designed in such a way that the strips will experience the strains which closely resemble the actual strain distribution in the critical area of the component. The sensor can be placed outside the notch but still would experience the same fatigue damage as the notch tip. The sensor is attached to the surface of structural member which is being monitored. The strips will fail in a sequential manner from the strip experienced the highest strain magnification to the lowest. Each strip failure corresponds to the particular fatigue damage accumulated by the structure being diagnosed. This information allows for predicting remaining component life[5-6]. A schematic of the fatigue sensor and its arrangement in a structure is shown in Figure 1.

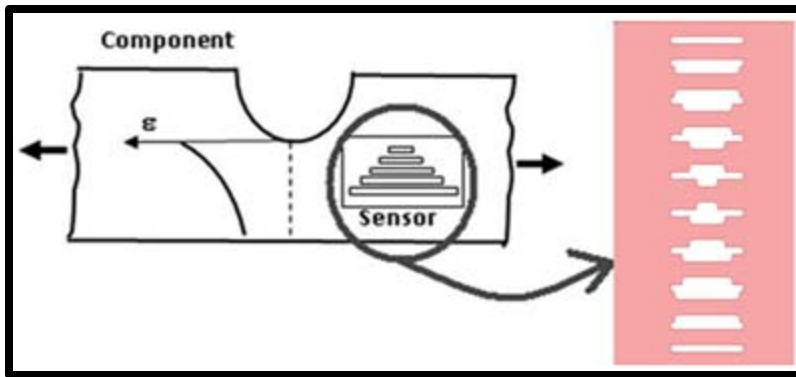


Figure 1: Fatigue gauge and its mounting configuration

One of the major advantages of the proposed sensor is that it can be deployed on any structure, whether new or old (already in service) provided the past stress cycle information or the loading history of the structure is known. Added to this, the fatigue sensor under consideration is designed in such a way that it can be placed at any portion on the component not necessarily at the high stress concentration zone but still would imitate the stress and strains at the critical region with a certain magnification.

The inset in Fig. 1 shows a schematic representation of an initial design of a fatigue sensing gauge. The gauge mainly comprise of a metallic coupon with alternate strips and slots. The strips in the sensor are called ligaments. As seen from the figure each ligament is divided into two parts with different areas of cross-section and the size of smallest area of cross-section (the active ligaments) are decreasing from ends to the center. The ligaments on either ends of the gauge with uniform area of cross-section are called reference ligaments. The strain in the reference ligament is related to the strain in the component where the gauge is placed. The strain ratio of each of the active ligament is a magnification of the strain in the reference ligament thereby relating to the strain in the critical location. When attached in an appropriate position of the component, the test gauge would experience the same strain history and ambience as that experienced by the test structure.

As the gauge is subjected to cyclic stress of known magnitude, each of the active ligaments will experience elongation or contraction equal to or larger than that experienced by the reference ligament. Active ligaments will experience different amounts of induced strains (ϵ) from the

same total elongation, as these active ligaments vary in length. Thus the amount of induced strains of each active ligament vary as a function of its length. By designing the length and area of cross-section dimensions of active ligaments they can experience a desired strain magnification. As a result each ligament will thus start to fail in the order from highest to lowest induced strain. Thus induced strains can be related to the service life of the structure and in this way the remaining service life or the expanded service life of the structure can be determined. Analytical basis for the design of the proposed fatigue gauge is discussed in the following section.

Analytical Modeling

Figure 2 shows a two ligament section of the fatigue gauge comprising of a reference and active ligament. In this case, the strain measurement is made with respect to the reference ligament 'R'. The dimensions of the actual active ligament are fixed relative to this reference. The reference and active ligaments along with the basic nomenclature of the parameters used in analytical modeling is represented in Fig.2. It may be noted that the practical gauge employed for the fatigue life measurement will have a reference ligament 'R' and a series of active ligaments with the actual number of these decided based on the specific design parameters. The active ligaments will have different lengths and areas of cross-section in the middle depending on the application. This basic configuration is considered for developing an analytical analysis. The arrows in Fig.3 refer to the loading / displacement direction.

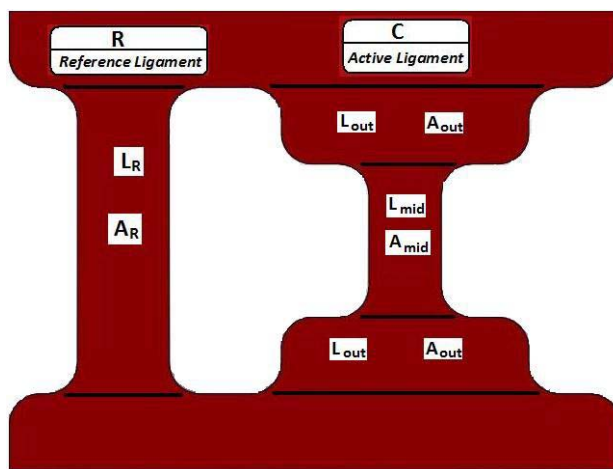


Figure 2 : Gauge with a reference and active ligament

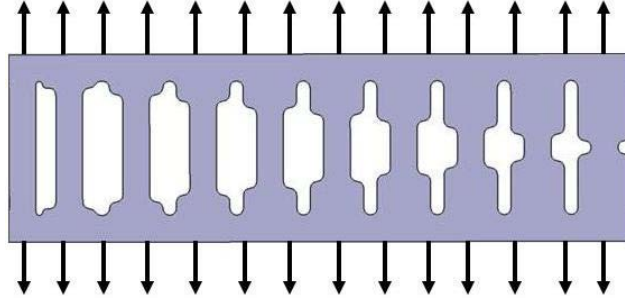


Figure 3: A schematic depicting the loading direction of the gauge

The strain analysis of our fatigue gauge design is based on three important assumptions. Firstly, the displacement experienced at the top and bottom ends of the gauges is expected to be the same in all ligaments i.e., $\Delta L_i = \text{constant}$. The gauge is considered to be made of the same material i.e., Young's modulus of all the ligaments is the same ($E_i = \text{constant}$). The final assumption is that the critical service strain is experienced in the longitudinal direction of the ligaments as shown in Fig. 3. The following is a derivation for the calculation of the ratio of elastic strain in the active ligament to the elastic strain in the reference ligament (see Fig.2)

The total length of the ligament is.

$$L = L_{out} + L_{mid} + L_{out} = L_R \quad (1)$$

$$\Delta L = \Delta L_R = \Delta L_{out} + \Delta L_{mid} + \Delta L_{out} \quad (2)$$

The strain in the reference ligament is calculated as

$$\epsilon_R = \frac{\Delta L_R}{L_R} = \frac{\Delta L_{out} + \Delta L_{mid} + \Delta L_{out}}{L} \quad (3)$$

The strain in the middle portion of the active ligament 'C' is

$$\epsilon_{mid} = \frac{\Delta L_{mid}}{L_{mid}} \quad (4)$$

From the above two equations (3) and (4) we have,

$$\frac{\epsilon_{mid}}{\epsilon_R} = \left(\frac{\Delta L_{mid}}{\Delta L_{out} + \Delta L_{mid} + \Delta L_{out}} \right) \left(\frac{L}{L_{mid}} \right) \quad (5)$$

Using Hooke's law, we have, $\Delta L = [(PL) / (AE)]$. Substituting the expression for ΔL in the equation (5) and modifying it, the expression for the ratio of the strain in the outer and middle part of each ligament to the strain in the reference ligament is obtained as :

$$\frac{\epsilon_{i,out}}{\epsilon_R} = \left(\frac{L}{L_{i,out}} \right) \left(\frac{\alpha_{i,out}}{\alpha_{i,out} + \alpha_{i,mid} + \alpha_{i,out}} \right) \quad (6)$$

$$\frac{\epsilon_{i,mid}}{\epsilon_R} = \left(\frac{L}{L_{i,mid}} \right) \left(\frac{\alpha_{i,mid}}{\alpha_{i,out} + \alpha_{i,mid} + \alpha_{i,out}} \right) \quad (7)$$

Where,

ϵ is the induced strain,

α is a shape factor i.e., ratio of length to the cross-sectional area of the ligament (L/A),

i is the ligament number (here $i = 1$ to 9),

L is the total length of the ligament, and

A is the cross-sectional area of the ligament.

The equations (6) and (7) are used to calculate the strain ratio of the outer and inner parts of each of the active ligaments to the strain in the reference ligament. The data in Table 1 shows the length of each part of all the nine active ligaments considered and the corresponding strain ratio of the middle portion and the outer portions of the active ligaments. The dimensions in Table 1 are in arbitrary units. The area of cross-section of the middle portion of all the nine active ligaments is 100 sq. units and that of the outer portions of all the active ligaments is twice the value of the middle portion.

	Length of the ligaments as input			Strain ratio as output	
	Outer	Middle	Outer	Outer	Middle
Ligament 1	5	90	5	0.52632	1.05263
Ligament 2	10	80	10	0.55556	1.11111
Ligament 3	15	70	15	0.58824	1.17647
Ligament 4	20	60	20	0.62500	1.25000
Ligament 5	25	50	25	0.66667	1.33333
Ligament 6	30	40	30	0.71429	1.42857
Ligament 7	35	30	35	0.76923	1.53846
Ligament 8	40	20	40	0.83333	1.66667
Ligament 9	45	10	45	0.90909	1.81818

Table 1: Length of the ligaments as input and the resulting strain ratios

The dimensions of the ligaments can be calculated based on the ratio of strain in the middle portion of the active ligaments to the strain in the reference ligament which in turn is related to the actual strain in the component. In other words, the dimensions of each of the active ligaments can be designed in such a way that they would fail after a certain percentage of the fatigue life of the component. Thus, knowing the desired strain magnification, it is possible to determine the dimensions of each of the active ligaments. Following this simple analysis, we derived an expression for calculating the length of the middle portion of the active ligaments based on the strain ratios, which is given by

$$L_{mid} = \left[\left(\frac{2L_R}{x} \right) - L_R \right] \quad (8)$$

The equation (8) can be attested for the same kind of gauge with nine active ligaments by substituting the values of strain ratio 'X' of middle ligaments (from Table 1). The lengths and cross-sectional values obtained are in agreement with the values shown in Table 1. In order to investigate the uniformity of strain distribution in active ligaments, the numerical simulations were performed.

Finite Element Analysis (FEA) Elastic Simulation

Numerical simulation of the fatigue gauge response was performed using commercially available software. The simulations were done assuming an elastic behavior of the material. The main objective of this analysis is to determine and identify the important design parameters and understand their effect on the strain experienced by different active ligaments. This also helps in optimizing different dimensional parameters of the designed gauge.

The important parameters identified in the designed gauge configuration are :

1. End geometry of the gauge
2. Symmetry of the gauge configuration
3. Fillet radius at the ends of the active ligaments

In particular, the effect of these parameters on the strain distribution across different ligaments is analyzed using the FEA simulations and these results are discussed further.

End geometry of the gauge

The 'end geometry' of the gauge configuration plays a significant role in obtaining proper strain distribution in the reference ligament. Figure 4 shows the strain distribution in the middle portion of the reference ligament. The vertical axis of the plot in Figure 4 shows the normal strain in Y-direction (i.e., the direction of the applied displacement) and the horizontal axis shows the width of the middle portion of the left reference ligament (Fig. 4). Different lines in the plot represent different total displacements applied in the range from 1 to 10 units. As observed from the graph, the strain distribution in the middle portion of the reference ligament is not uniform throughout the width. The maximum strain concentration is at outer ends of the ligament and decreasing towards the inner end of the reference ligament, which is not desirable. Since we would want to relate the strains in each of the active ligament to the strain in the component via the strain in the reference, it is critical that the strain distribution be almost uniform throughout the length of the reference ligament.

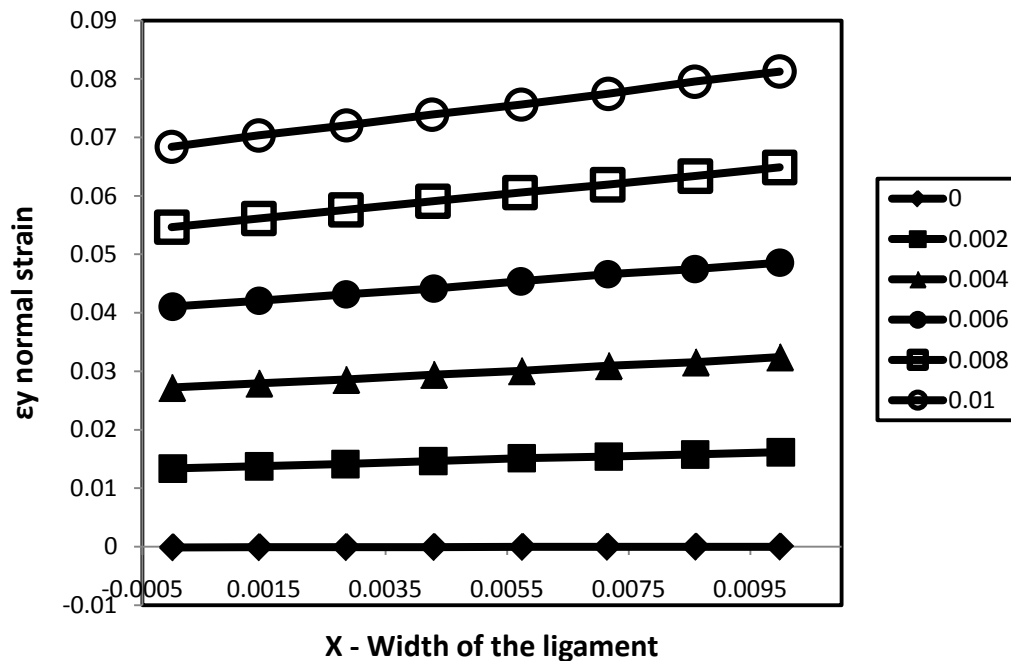


Figure 4: Strain distribution in reference ligament

However, it may be observed that the range of strain variation across the width is decreasing as the applied displacement is decreased. To reduce the strain variation in the middle portion of the reference ligament, another reference ligament is added adjacent to the existing one.

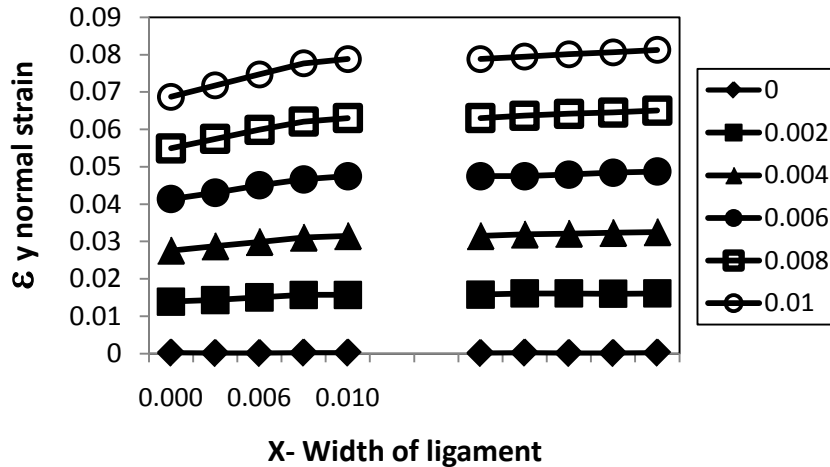


Figure 5: Strain distribution in the reference ligaments

In Figure 5, the left half of the plot shows the strain distribution in the outermost reference ligament, while the right half of the plot depicts strain distribution in the middle portion of the second reference ligament. It may be seen from the Fig. 5 that the strain distribution in the middle portion of the second reference ligament is more uniform compared to the first reference ligament. Hence, we consider the second reference ligament for the calculations and analysis while dealing with the strain ratios. From Figures 4 and 5, it is clear that the end geometry (one or two reference ligaments) of the gauge play a very important role in obtaining a more uniform strain distribution in the reference ligaments.

Symmetry of the gauge

Another important parameter in the design of the fatigue gauge is the double symmetry. The strain analysis discussed in the previous section used a gauge (shown in figure 3) that does not conform to a double symmetrical geometry.

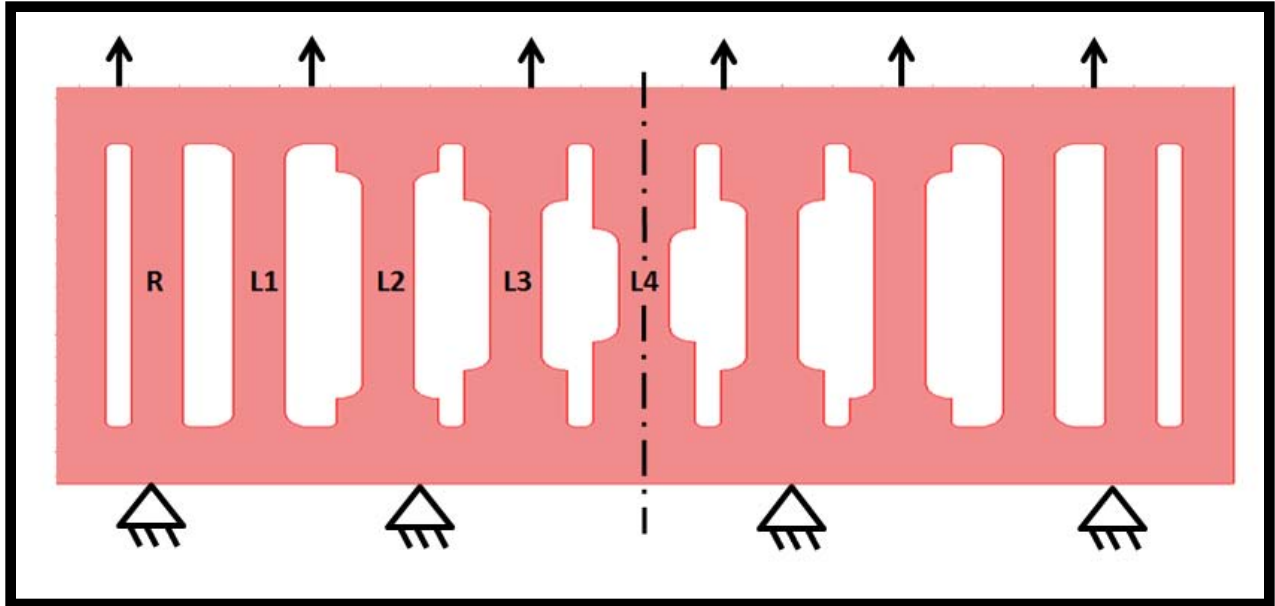


Figure 6: Double symmetry design

Figure 6 shows a schematic of the gauge with a double symmetrical arrangement. Another important modification that is incorporated in the design includes the consideration of active ligaments with the decreasing order of the length of the middle portion of the ligaments (ligament 1 to 4).

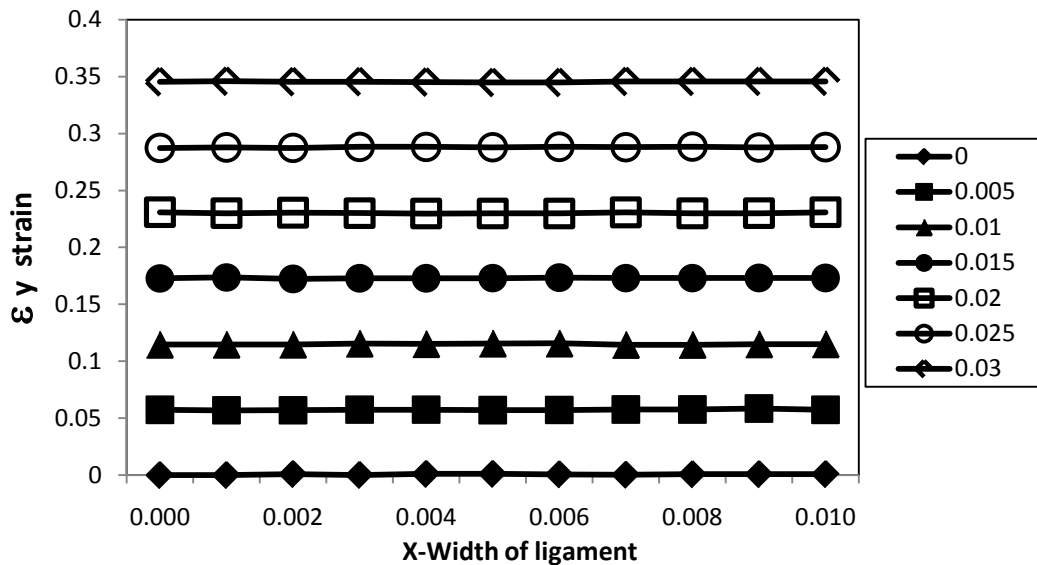


Figure 7: Strain distribution in ligament 4

Figure 7 shows the strain distribution in the middle portion of the ligament 4 in the gauge with double symmetry as in Figure 6. This shown quite uniform strain over the entire width of the

ligament, which is ideal for the operation of the fatigue gage. The other parameter that was analyzed is the aspect ratio (ratio of length to width of ligament in the middle portion). It has been observed that for lower aspect ratios the maximum strain concentration was predominantly confined to the sides of the ligament as against for the ones with larger aspect ratio. The results of the effect of the aspect ratio have not been presented as these did not seem to be as crucial as the others.

Fillet radius

Fillet radius is the other important parameter, which has significant influence on the strain distribution of the active ligaments within the gauge. In this context, the gauges with symmetry about ligament 4 are considered. Figures 8 and 9 show the symmetry designs with fillet radii of 5 and 20 units respectively.

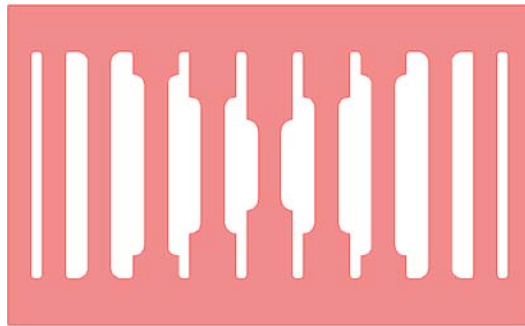


Figure 8: Symmetry design with a fillet radius of 5 units

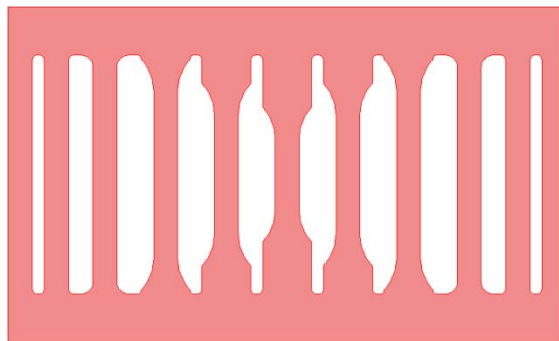


Figure 9: Symmetry design with fillet radius of 20 units

The results of the finite element simulations for the above two gauges are shown below. Figure 10 shows the strain distribution and the deformation of the gauge with a fillet radius of 5 mm

while Fig. 11 shows the deformation and the strain distribution of the gauge with a fillet radius of 20 units.

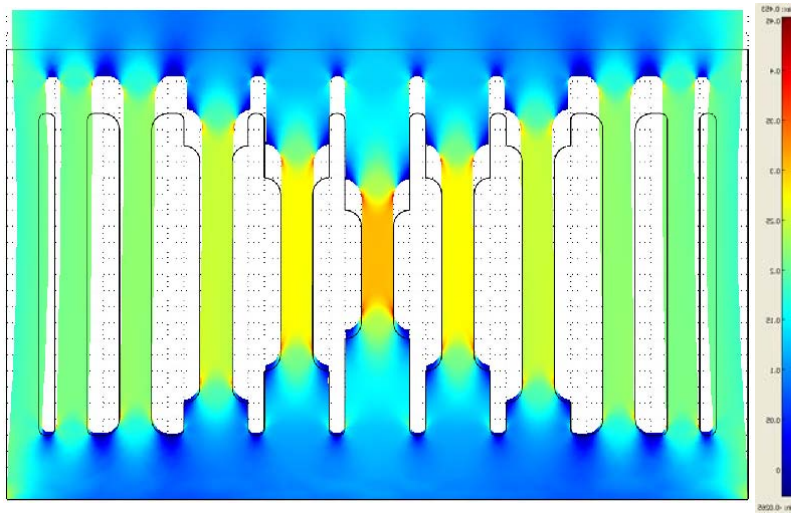


Figure 10: Deformation and strain distribution for 5 units fillet radius

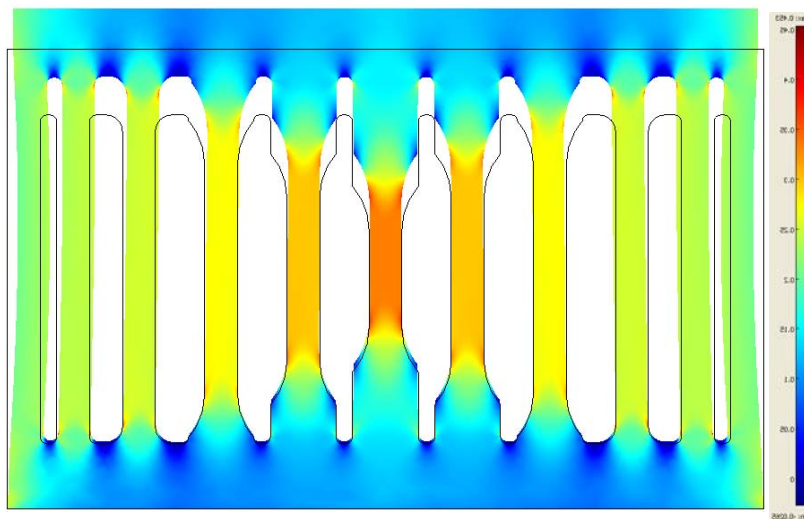


Figure 11: Deformation and strain distribution for 20 units fillet radius

From Fig. 10, it can be seen that there is a maximum strain concentration at the corners of the middle portion of the ligaments due to which the ligament would fail first at the corners. In contrast, the Fig. 11 shows a much uniform distribution of the strain in the middle portion and hence the failure of the ligament occurs in that region. The strain at the fillet is 30% higher compared to the strain observed at the middle of the ligament for the gauge with smaller radius while it is only 12% for the larger fillet. From the above results, it can be concluded that the fillet

radius also plays an important role in the design of the strain gauge and from this simulation it clearly shows that larger fillet radius is more desirable for proper fatigue diagnosis.

Prototype single ligament testing and results

As pointed out earlier, the fatigue sensor could be placed at any location on the component not necessarily at critically stressed region but would still be able determine the strains at a critical location with known magnification (strain ratio). Finite element analysis (FEA) simulations were performed on the fatigue sensor to obtain the strain ratios of each of the active ligaments i.e., the ratio of strain in each of the active ligament to the strain in the reference ligament. The simulation were done using commercial FEA software. The strain ratios were calculated based on the strain values taken from the mid-point of each of the active ligaments and reference ligament shown by yellow dots in the Figure 12. The nodes resulted after meshing the sensor and the loading pattern applied on the fatigue sensor are also seen in the Figure 12. The strain ratios obtained for each of the four active ligaments are shown in Figure 13.

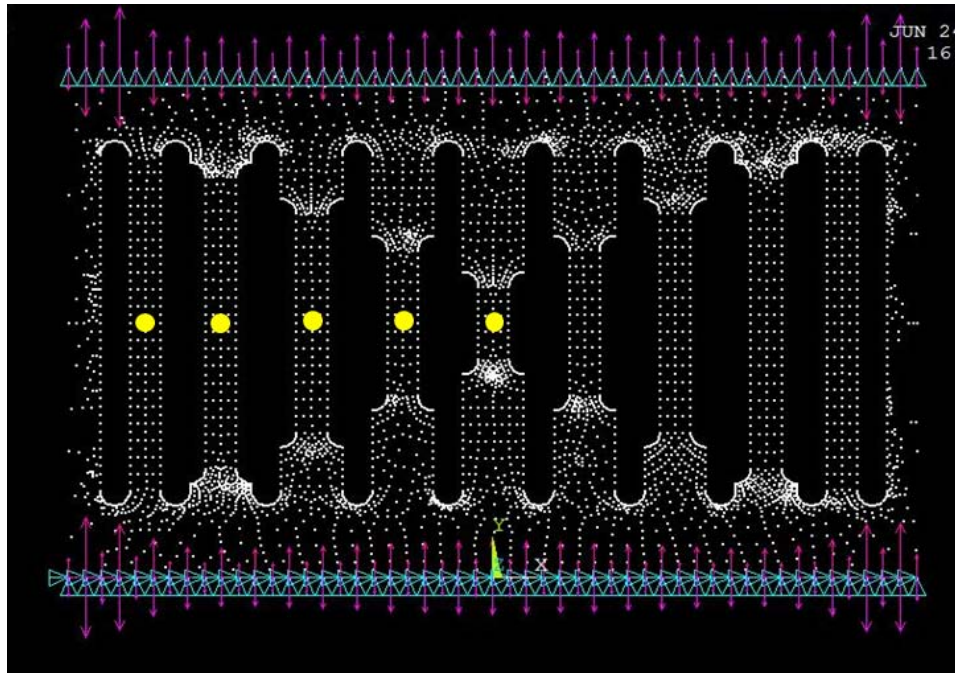


Figure 12: Screenshot of meshed sensor.

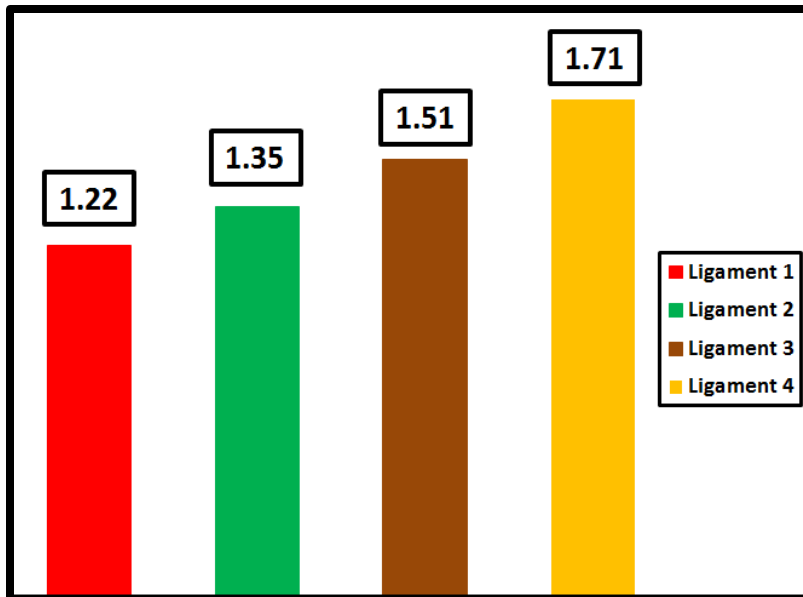


Figure 13: Strain ratios for the active from the FEA simulation (elastic)

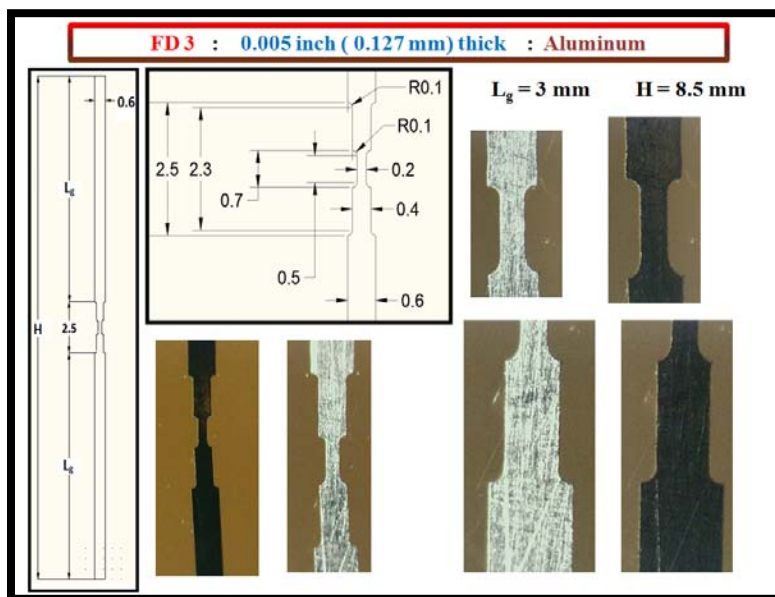


Figure 14: The figure showing the pictures and dimensional details of 0.005" Aluminum single ligament

The strain ratio variation of the ligaments and its effective relationship with a notch on a test specimen were investigated by designing a single ligament with specific strain ratio. This was subjected to tensile testing by fixing it on a specimen with a notch having similar strain ratio. These single ligaments were tested for the validity of the working principle of the sensor i.e., the

sensor (in this case it is the single ligament) would break in the center region when placed on the component at a region away from a stress concentration zone when it undergoes cyclic loading. This single ligament testing has been done on 0.005” thick aluminum samples. The single ligaments were fabricated using micro-wire electro-discharge machining (μ w-EDM), as shown in figure 14. A notch is cut on the test specimen onto which the sensor ligament is attached. This notch would simulate the stress concentration zone when the specimen is subjected to cyclic loading and hence act as the source for crack initiation. The sharp v-notch cut on the backing specimen has a depth of 5mm which is calculated on the basis of taking the strain ratio of the single ligament as the stress concentration factor of the notch [16]. The strain ratio obtained corresponds to the stress-strain behavior of the single ligament in the elastic region. For this reason, ligament is placed on the backing specimen in a region where the stress distribution is uniform. FEA simulations were done on the notched specimen for determining the location for attaching the single ligament on the specimen. The stress distribution across the width of the specimen at different locations (going vertically from the notch plane) is evaluated by simulating a uniform tensile load on the specimen. Figure 15 shows the stress distribution across the width of the specimen at the notch plane (black line) and at a location 5mm above the notch plane (green line), which were obtained in the above simulation. It can be seen that at a distance of 5mm (vertically) from the notch plane, the stress distribution across the width of the specimen is uniform and this region of the specimen is in elastic region.

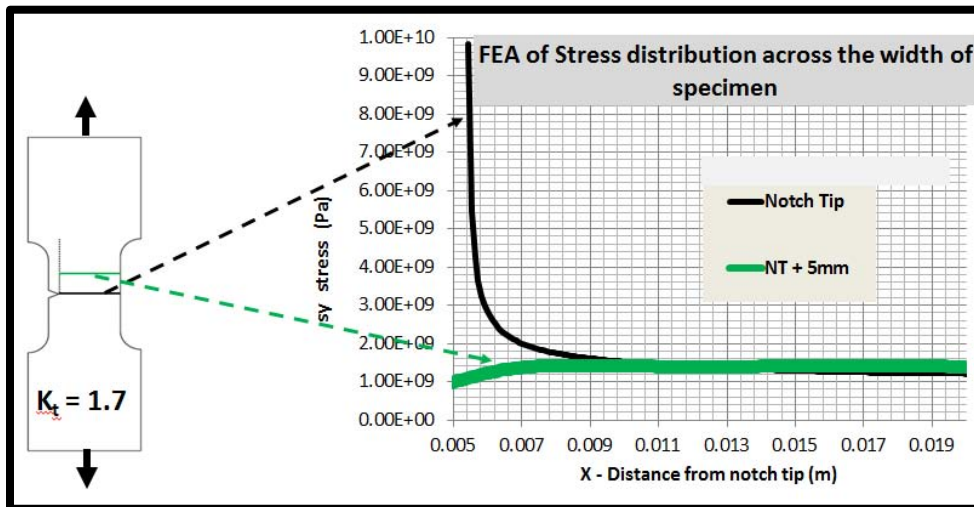


Figure 15: Stress distribution across the width of the backing specimen

Prior to performing the cyclic loading on the ligament, it is necessary to determine the yield strength of the specimen material used. Hence, the specimen was subjected to tensile testing and plotted the stress-strain curve. The yield strength of the material is found to be around 5500 N. Based on this value obtained, the cyclic loading parameters were determined. A set of 5 specimen were prepared with 0.005” thick aluminum single ligaments attached at the prescribed locations on each of them. The five specimen were subjected to cyclic loading using a tensile testing machine. These were subjected to 5 different loads, i.e., 5000 N, 4500 N, 4000 N, 3500 N and 3000 N respectively. The stress ratio and the frequency of the cyclic loading in each case was (-)0.5 and 1 Hz respectively. The potential drop method was employed for testing the single ligaments which provided the corresponding crack length data as the crack propagates with increasing number of cycles. The specimen has also been observed with a high magnification tele-microscope for the crack initiation in the backing specimen and the breaking of the ligament. Figure 16 shows the Load vs. number of cycles plot with load on the specimen on the vertical axis and number of cycles on horizontal axis.

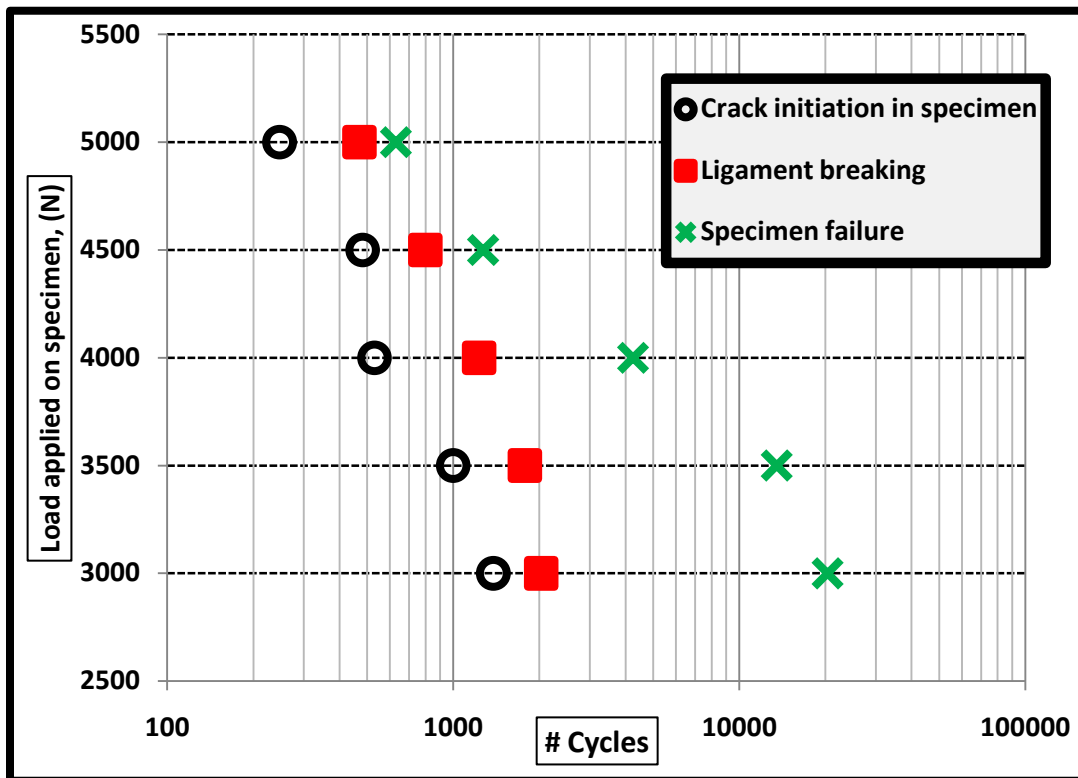


Figure 16: Results from the single ligament testing

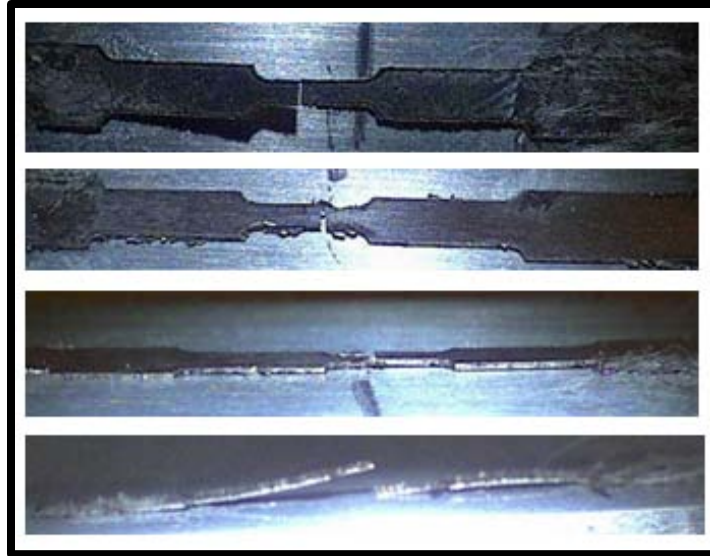


Figure 17: The pictures of broken single ligaments due to cyclic loading

For each specimen (i.e., for each load applied), number of cycles of the cyclic loading have been plotted for the crack initiation in the specimen at the notch tip, ligament breaking and the complete specimen failure. It is evident from the plot that for higher loads, there is not much fatigue life between the crack initiation and complete failure. The ligament breaks at cycles closer to specimen failure. On the other hand, as the applied loads decreased, the number of cycles at which the ligament breaks is closer to the crack initiation and the time between the ligament breaking and the specimen failure increases. This indicates that there is still enough time for repairing or replacing the component well ahead of the complete failure.

Summary

This paper presented the concept of a standalone fatigue gauge, that can provide a direct indication of the fatigue life of a given structural component. Analytical basis for the design of such a sensor is established using simple geometrical and mechanical considerations. Design simulations were carried out using commercially available finite element software. These numerical simulations helped us in arriving at an optimal design, in terms of achieving uniform strain distribution on different ligaments of the designed sensor. Further, this study identified three important parameters viz., end-geometry effects, symmetry of the sensor ligament configuration and the fillet radius of the active ligaments. The strain distribution in the active

ligaments with respect to these parameters is studied in detail. The effect of having an extra reference ligament on either ends of the gauge along with the existing ones resulted in uniform strain distribution in the inner reference ligaments. As a result, the final layout of the fatigue sensor has a symmetry about the smallest ligament in the design. A single ligament sensor was fabricated using micro-Wire Electro-discharge machining method and subjected to cyclic loading to evaluate the accuracy of simulation results. These studies showed that the component (backing specimen) failure follows the breaking of the single ligament that is placed away from the notch tip. Enough time lag between the ligament breaking and the complete failure of the backing specimen always ensures pre-warning of an impending catastrophic failure that can be prevented without any major consequences.

References

1. C. M. Suh, R.Y., H. Kitagawa, *Fatigue Microcracks in a low carbon steel*. Fatigue & Fracture of Engineering Materials & Structures, 1985. **8**(2): p. 193-203.
2. S. Beretta, P.C., *Microcrack Propagation and Microstructural Parameters of Fatigue Damage*. Fatigue & Fracture of Engineering Materials & Structures, 1996. **19**(9): p. 1107-1115.
3. K. J. MILLER, M.F.E.I., *Damage Accumulation During Initiation and Short Crack Growth Regimes*. Fatigue & Fracture of Engineering Materials & Structures, 1981. **4**(3): p. 263-277.
4. Harting D.R., *The S-N Fatigue life gauge: A Direction means of measuring cumulative fatigue damage*. Experimental Mechanics, 1996. **6**(2): p. 19-24.
5. Taylor D., *The theory of critical distances*. 2007, Elsevier Publishers, Oxford, UK..
6. Taylor D., B.P. BelKnani K, *Prediction of fatigue failure location on a component using a critical distance method*. International Journal of Fatigue, 2000. **22**: p. 735-42.
7. Crites N.A., *Fatigue Indication*. 1974, Battelle Memorial institute, Columbus, OH: USA, Patent # 3786679.

8. Henkel D.P., *Remote and powerless miniature fatigue monitor and method*. 1996: USA, Patent # 5531123.
9. Howard Warren Smith I., *Fatigue Damage Indicator*. 1976, The Boeing company, Seattle: USA, Patent # 3979949.
10. John M. Papazian, J.N. Robert P. Silberstein, Greg Welsh, David Grundy, Chris Craven, Leslie Evans, Neil Goldfine, Jennifer E. Michaels, Thomas E. Michaels, Yuanfeng Li, Campbell Laird, *Sensors for monitoring early stage fatigue cracking*. International journal of fatigue, 2007.**29**: p. 1668-1680.
11. Kwon Y.W., *Fatigue Measurement Device and Method*. 2006: USA, Patent # US 6983660 B2.
12. Masatoshi Kuroda S.Y., Koji Yamada, Yoshihiro Isobe, *Detection of Plastic deformation and Fatigue Damage in Pressure vessel steel by leakage Magnetic Flux Sensors*. Material Science Research International, 2001.**7**(3): p. 213-218.
13. Maurice A. Bruli, H.P., *Method of making a device for monitoring fatigue life*. 1987, Tensidyne Scientific Corporation, Horsham, PA: USA, Patent # 4639997.
14. Thomas, E.D.R., *Fatigue sensors*. 1974, Hawker Siddeley Aviation Limited, Surrey, England: USA, Patent # 3782178.
15. Zhou Zhi, D.Z., JiaZhonghui, OuJinping, *New kind of Structural Fatigue life prediction smart sensor*. Smart structures and materials, 2004: p. 324-331.
16. Noda, N. A., Sera, M., Takase, Y., *Stress concentration factors for round and flat test specimens with notches*, Int. J. Fatigue, 1995. 17(3): p. 163-178.
17. <http://www.vishay.com/docs/11521/crackpro.pdf>